

MICROCOPY RESOLUTION TEST CHART  
NATIONAL BUREAU OF STANDARDS-1963-A



Division of Engineering  
BROWN UNIVERSITY  
PROVIDENCE, R. I.

Engineering Materials Research Laboratory

(12)

AD A1 24993

48 HOUR MULTIAXIAL CREEP AND  
RECOVERY OF 2618 ALUMINUM  
ALLOY AT 200°C

Jow-Lian Ding  
William N. Findley

DTIC  
SELECTED  
MAR 1 1983  
S  
A

This document has been approved  
for public release and sale; its  
distribution is unlimited.

U.S. Army Research Office  
Technical Report No. 1  
Grant DAAG 29-81-K-0138

DTIC FILE COPY

ARO DAAG 29-81-K-0138/1  
EMRL-87 88 02 028 057

October 1982

UNCLASSIFIED

SECURITY CLASSIFICATION OF THIS PAGE (When Data Entered)

REPORT DOCUMENTATION PAGE		READ INSTRUCTIONS BEFORE COMPLETING FORM
1. REPORT NUMBER Technical Report No. 1	2. GOVT ACCESSION NO. AD A724 993	3. RECIPIENT'S CATALOG NUMBER
4. TITLE (and Subtitle) "48 HOUR MULTIAXIAL CREEP AND RECOVERY OF 2618 ALUMINUM ALLOY AT 200°C"	5. TYPE OF REPORT & PERIOD COVERED Technical	
	6. PERFORMING ORG. REPORT NUMBER EMRL 87	
7. AUTHOR(s) Jow-Lian Ding and William N. Findley	8. CONTRACT OR GRANT NUMBER(s) Grant No. DAAG29-81-K-0138	
9. PERFORMING ORGANIZATION NAME AND ADDRESS Division of Engineering, Brown University, Box D Providence, RI 02912	10. PROGRAM ELEMENT, PROJECT, TASK AREA & WORK UNIT NUMBERS	
11. CONTROLLING OFFICE NAME AND ADDRESS U. S. Army Research Office Post Office Box 12211 Research Triangle Park, NC 27709	12. REPORT DATE October 1982	
	13. NUMBER OF PAGES 37 pages	
14. MONITORING AGENCY NAME & ADDRESS (if different from Controlling Office)	15. SECURITY CLASS. (of this report) Unclassified	
	15a. DECLASSIFICATION/DOWNGRADING SCHEDULE	
16. DISTRIBUTION STATEMENT (of this Report)  Approved for public release; distribution unlimited.		
17. DISTRIBUTION STATEMENT (of the abstract entered in Block 20, if different from Report)  NA		
18. SUPPLEMENTARY NOTES The view, opinions, and/or findings contained in this report are those of the author(s) and should not be construed as an official Department of the Army position, policy, or decision, unless so designated by other documentation.		
19. KEY WORDS (Continue on reverse side if necessary and identify by block number) Multi-axial Creep, Creep, Creep of Aluminum Alloy, viscous-viscoelastic model, aging, strain recovery, compression creep, Tresca relation.		
20. ABSTRACT (Continue on reverse side if necessary and identify by block number) Data are reported from 48 hour constant multiaxial stress creep followed by 48 hour recovery with the magnitudes of the effective stress ranging from 34.5 MPa (5.00 ksi) to 175.5 MPa (25.46 ksi). They differed from a previous data set in the much longer constant-stress durations and the inclusion of data from low stress creep, compression creep and short term aging tests. Data were represented by a viscous-viscoelastic model in which the time-dependent strain was resolved into recoverable and nonrecoverable components. Previous stress-strain relations for constant stress creep and recovery were modified to		

DD FORM 1 JAN 73 1473 EDITION OF 1 NOV 65 IS OBSOLETE

UNCLASSIFIED

SECURITY CLASSIFICATION OF THIS PAGE (When Data Entered)



48 Hour Multiaxial Creep and Recovery  
of 2618 Aluminum Alloy at 200°C

by

Jow-Lian Ding<sup>1</sup>

and

William N. Findley<sup>2</sup>

<sup>1</sup>Research Assistant, Division of Engineering  
Brown University, Providence, RI 02912

<sup>2</sup>Professor of Engineering, Division of Engineering  
Brown University, Providence, RI 02912

U.S. Army Research Office  
Technical Report No. 1  
Grant DAAG-29-81-K-0138

Division of Engineering  
Brown University  
Providence, R.I. 02912

October 1982

Approved for Public Release; Distribution Unlimited

The view, opinions and/or findings contained in this report are those of the authors and should not be construed as an official Department of the Army position, policy, or decision unless so designated by other documentation.

## Table of Contents

	<u>Page</u>
Abstract	1
Introduction	1
Material and Specimen	3
Experimental Apparatus and Procedure	3
Experimental Results	4
Analysis of the Creep and Recovery Data	5
Symmetry in Tension and Compression	9
Aging Effects	10
Creep Rates and Creep Surfaces	10
The Stress Dependence of $\epsilon^{VE}$ and $\epsilon^V$	14
Conclusions	18
Acknowledgement	19
References	20
Table 1 - Chemical Compositions of the Previous and the Current Lots of 2618-T61 Aluminum Alloy	22
Table 2 - Numerical Results for 2 Hour Creep and Recovery Data	23
Table 3 - Numerical Results for 48 Hour Creep and Recovery Data	24
Table 4 - Constants for Eq. (7) and (8)	25
Figure Captions and Figures	26-37

## ABSTRACT

Data are reported from 48 hour constant multiaxial stress creep followed by 48 hour recovery with the magnitudes of the effective stress ranging from 34.5Mpa(5.00ksi) to 175.5Mpa(25.46ksi). They differed from a previous data set in the much longer constant-stress durations and the inclusion of data from low stress creep, compression creep and short term aging tests. Data were represented by a viscous-viscoelastic model in which the time-dependent strain was resolved into recoverable and nonrecoverable components. Previous stress-strain relations for constant stress creep and recovery were modified to include the current experimental observations of the nonexistence of creep limits, negligible aging effects, and symmetry in tension and compression. The time dependence was represented by a power of time with different exponents for the recoverable and nonrecoverable components. A homogeneous function of maximum shear stress was developed to represent the full range of stress dependence of the nonrecoverable time dependent components; and the third order multiple integral representation was used for the recoverable component.

## INTRODUCTION

Past experimental work in creep under multiaxial stress was reviewed in [1].

In previous work at Brown University on 2618-T61 aluminum alloy [2-5] , a constitutive relation in which the total strain was decomposed into elastic, time-independent plastic, viscoelastic, and the time-dependent nonrecoverable components was based on a series of short time (2 h), relatively high stress creep tests with different creep and recovery durations, see [2] . It was reported that there appeared to be creep limits below which the creep strains did not occur or were negligible. It was also shown that the two time-dependent strain components had the same time dependence and their relative proportion might be taken to be independent of stress.

In the present work, a series of constant duration creep and recovery tests were performed whose stress levels were evenly distributed from those causing little creep strain in 48 hours to those causing tertiary creep in less than one hour. They were used not only to check the behavior below the apparent creep limits but also to check the applicability of previous results to longer term primary creep. Two aging tests were also performed to study the aging effects within the time span of the tests performed. And two compression tests were used to compare the creep behavior in tension and compression. The purposes of this work were to refine and to extend the viscous-viscoelastic constitutive relations and to provide a systematic data basis for other theoretical approaches and for more understanding of multiaxial creep behavior.

In subsequent papers, data for variable states of stress will be presented together with predictions based on the present data using two different types of constitutive relations with different hardening natures.

#### MATERIAL AND SPECIMEN

The material employed in the present work was aluminum forging alloy 2618-T61 which was the same kind of material as that in previous work [2-6] , but obtained 14 years later from the same source, possibly from the same batch. The chemical composition of the current batch was examined and compared with that of the old batch. The small deviations shown in Table 1 may be negligible.

Specimen were thin-walled tubes of circular cross section machined from 63.5mm dia. extruded rod. The nominal outside diameter, wall thickness and gage length were 25.4, 1.52 and 101.6mm (1.00, 0.06, and 4.00 in), respectively. A more complete description of material and specimen is given in [2] .

#### EXPERIMENTAL APPARATUS AND PROCEDURES

The combined tension and torsion creep machine used in these experiments and the procedures for performance and data acquisition were described in [2-7] .

A compression machine employed in the present work was described in [8] .

The temperature control and measurement systems were the same for both machines described in [2-8] . Except for aging tests, the specimen was soaked at the test temperature of 200°C for approximately 18 hours prior to testing. All experiments were performed at a test temperature of 200°C. The variation of temperature was within  $\pm 0.30^\circ\text{C}$  both with time and position.

#### EXPERIMENTAL RESULTS

The test numbers and the stress levels under which the creep steps were performed are shown in Fig. 1. The magnitudes of the stress levels are given in Table 2. Three Mises stress curves whose magnitudes of effective stress defined by  $\sigma^2 + 3\tau^2 = (\sigma_{\text{eff}})^2$  for combined tension  $\sigma$  and torsion  $\tau$  stresses can be constructed through these stress points. The magnitudes of the three effective stresses are 109.5Mpa (15.88ksi), 137.2Mpa (19.90ksi), and 175.5Mpa (25.46ksi), respectively. One Tresca curve defined by  $\sigma^2 + 4\tau^2 = (82.7 \text{ MPa})^2 [(12.00 \text{ ksi})^2]$  can also be constructed through these stress points. Each combined tension and torsion test was interrelated with at least one pure axial creep test and one pure shear test. The test durations were all 48 hours for both creep and recovery except for test 42 whose creep step only lasted for 36.02 hours with a recovery

step of 36 hours.

All the creep and recovery data are shown in Fig. 2 through 6 in which symbol A represents pure axial tests; symbol T represents pure shear tests and symbols CA and CT represent the axial and the shear strains respectively in combined tension-torsion tests. Fig. 6 shows that the effective stress of 175.5 Mpa(25.46ksi) was high enough to cause tertiary creep in less than one hour.

#### ANALYSIS OF THE CREEP AND RECOVERY DATA

In the viscous-viscoelastic model, the total strain was decomposed into elastic( $\epsilon^E$ ), plastic( $\epsilon^P$ ), viscoelastic ( $\epsilon^{VE}$ ), and time-dependent nonrecoverable( $\epsilon^V$ ) components. These components were taken to be independent of each other and additive.

In current work, the total strain  $\epsilon_{ij}$  was well represented by the expression:

$$\epsilon_{ij} = \epsilon_{ij}^{\circ} + \epsilon_{ij}^{+} t^N, \quad (1)$$

where  $t$  is time and  $\epsilon_{ij}^{\circ}$  and  $\epsilon_{ij}^{+}$  are stress dependent. The time dependence in this expression was satisfactory for representing the primary stage of creep.

Considering both the time-dependent strain components  $\epsilon^{VE}$  and  $\epsilon^V$  to be represented by power functions of time with different stress dependences, the total strain during creep

was expressed as:

$$\epsilon_{ij} = \epsilon_{ij}^E + \epsilon_{ij}^P + \epsilon_{ij}^{+VE} t^{n_1} + \epsilon_{ij}^{+V} t^{n_2} . \quad (2)$$

The strain during recovery from creep at constant stress for time  $t_1$  was the following according to the superposition principle,

$$\epsilon_{ij} = A_{ij} + \epsilon_{ij}^{+VE} \{t^{n_1} - (t-t_1)^{n_1}\} , \quad (3)$$

where  $A_{ij}$  is equal to  $\epsilon_{ij}^{+V} t_1^{n_2} + \epsilon_{ij}^P$ ,  $t_1$  is the creep duration, and  $\epsilon^V$  is by definition not recoverable.

The elastic strain during load removal was

$$\epsilon_{ij}^E = \epsilon_{ij}|_{t=t_1} - A_{ij} - \epsilon_{ij}^{+VE} t_1^{n_1} , \quad (4)$$

where the first term came from the creep data and the last two terms were obtained from the recovery data.

In order to obtain the most accurate values of the instantaneous responses upon loading and unloading, only the first two hours of creep and recovery data were used to compute  $\epsilon_{ij}^*$  in equation (1) and  $\epsilon_{ij}^E$  in equation (4). For test 42, only the data within 0.808 hours was used. The results are shown in Table 2 and the instantaneous responses are plotted in Fig.7 except for the value of  $\epsilon_{ij}^E$  for test 42 which was erratic. The average values of  $N$  and  $n_1$  in Table 2 are 0.301 and 0.229 respectively.

The data distribution shown in Fig.7 is nearly linear which implies that time-independent plastic strain

components are small or zero. Neglecting tests 40 and 42 because of their deviations in  $\epsilon_{ij}^E$  and  $\epsilon_{ij}^o$ , the inverse slopes of the best fitting straight lines yield the elastic moduli for tension  $E$  and for torsion  $G$  of  $6.50 \times 10^4$  Mpa ( $9.43 \times 10^3$  ksi) and  $2.38 \times 10^4$  Mpa ( $3.45 \times 10^3$  ksi) respectively, which are consistent with previous findings [2].

The recoverable viscoelastic component  $\epsilon^{VE}$  was determined from the recoverable data by using Eq. 3. Neglecting tests 40 and 42, the time exponent  $n_1$  was found to be independent of stress, as in [2], and the average value was  $n_1 = 0.223$ , see Table 3. This value of  $n_1$  was nearly the same (0.244) as previously determined [2].

To determine the nonrecoverable time-dependent components  $\epsilon^V$ , the recoverable strain  $\epsilon^{VE}$  was first subtracted from the creep data using the relation  $\epsilon_{ij}^{VE} = \epsilon_{ij}^{+VE} t^{0.223}$ . Before calculating the  $\epsilon^V$  components, the data in the secondary and tertiary stages were first eliminated because these stages were not described by Eq. 1. The cut-off point for primary creep was taken to correspond to a shear strain of the  $\epsilon^V$  component equal to 0.08 percent. The shear strain of  $\epsilon^V$  under combined tension and torsion stress states was defined by  $[\left(\frac{3}{4}\epsilon_{11}^V\right)^2 + (\epsilon_{12}^V)^2]^{\frac{1}{2}}$  with incompressibility of  $\epsilon_{ij}^V$  and coincidence of the strain rate direction with the stress deviator assumed, as discussed in a later section. The cut-off times corresponding to this

criterion are given in the note for Table 3. The criterion resulted from the following considerations: Since Eq.(3) could describe very well the whole recovery data even for those tests in which secondary and tertiary stages showed up, see Fig. 5 and 6, it appeared that  $\epsilon^V$  dominated in these stages. So the criterion was based only on  $\epsilon^V$ .

The creep data in the primary stage, after subtracting  $\epsilon^{VE}$ , were used in Eq.2 to determine  $\epsilon_{ij}^{+V}$  and  $n_2$ , see Table 3. The exponent  $n_2$  was found to be independent of stress, as in [2], and to have an average value of 0.496.

The primary creep data were also fitted by Eq.1 to obtain  $\epsilon_{ij}^+$  and  $N$ , see Table 3. The average  $N$  was found to be 0.407. The results obtained through the above procedures are plotted in Fig. 2-6 in which Eq. (2) and (3) are represented by solid lines for creep and recovery data respectively and Eq. (1) is represented by dotted lines for creep data only.

Unlike results in previous work [2], the values of  $n_1$  and  $n_2$  were found to be different, even though both were independent of stress. Contrary to the results for 304 stainless steel [9,10], increasing the time period of creep data employed in analysis had the effect of increasing the time exponents; compare the values of  $N$  in Table 2 with those in Table 3. However, the value of  $n_1$  (recoverable) was nearly independent of the time duration of data employed,  $n_1=0.229$  and  $0.223$  for 2 and 48 hours

respectively. The exponent  $n_2$  was independent of stress even for the primary part of tests which subsequently showed secondary and tertiary stages. The value of  $n_2$  may be satisfactory for the entire primary stage (generally more than 48 hours for low stress tests) as long as aging effects are negligible.

The small differences between the instantaneous responses determined from 2 hours and 48 hours of data for a few high stress tests will be neglected in the subsequent analysis, and the values obtained from 2 hours of data will be used. This will cause small discrepancies between the experimental data and the theoretical predictions at the very beginning of a few high stress tests.

#### SYMMETRY IN TENSION AND COMPRESSION

Only a few data, see [11] pages 257-261, have been published for compression creep. These data showed that short term creep is symmetrical in tension and compression. Comparing the curves for tests 32 and 37, 39 and 44, also the corresponding values of  $\epsilon_{ij}^+$ ,  $\epsilon_{ij}^{+VE}$  and  $\epsilon_{ij}^{+V}$  in Table 3, shows that the total creep strains are close to each other in tension and compression throughout the test durations (the compression strains are some what greater than the tension). The viscoelastic components of strain  $\epsilon^{VE}$  in tension are a little higher than those in compression which results in larger strain for the  $\epsilon^V$

component in tension. This may be the true material behavior. However, because the differences did not increase with stress and the proportion of the viscoelastic component in the total strain is small, the differences will be neglected. This will induce deviations between the experimental data and theoretical predictions of about, 10% for  $\epsilon^{VE}$  and 5% for  $\epsilon^V$  in the viscous-viscoelastic model. Symmetry is not expected through the secondary and tertiary stages for constant load creep tests, see [11] , p258.

#### AGING EFFECTS

Two aging tests were performed in the current work. The pre-test soaking durations were 312 hours and 114 hours for tests 35 and 43 respectively. The whole test durations for nearly all the tests performed in the current research are within this range.

Comparing test 35 (aged 312 h) with test 32 (aged 18h) at the same stress; and test 43 (aged 114 h) with test 39 (aged 18 h) at the same stress show that there are no significant aging effects within 300 hours. However, a previous test reported in [2] showed that aging for 1103 hours had a considerable softening effect.

#### CREEP RATES AND CREEP SURFACES

A widely used representation for the multiaxial primary

creep rate is

$$\dot{\epsilon}_{ij} = F_a(J_2)\sigma'_{ij}t^m \quad (5)$$

where  $\sigma'_{ij}$  is the stress deviator and  $J_2$  is the second invariant of the stress deviator, see [12,13]. This expression implies that the creep deformation is incompressible and the creep rate tensor has the same direction as the applied stress deviator, that is, normal to the Mises surface. Furthermore, taking squares of both sides of (5) yields  $\frac{1}{2}\dot{\epsilon}_{ij}\dot{\epsilon}_{ij} = [F_a(J_2)]^2(\frac{1}{2}\sigma'_{ij}\sigma'_{ij})t^{2m}$ , where  $\frac{1}{2}\sigma'_{ij}\sigma'_{ij} = (J_2)^2$ . Thus the magnitude of the strain rate tensor defined by  $(\frac{1}{2}\dot{\epsilon}_{ij}\dot{\epsilon}_{ij})^{1/2}$  is constant along a Mises stress surface at a given time. In previous work [6,14,15], the creep surface was defined as the stress surface for which creep rate tensors had equal magnitudes following creep for a given time at constant stress. If eq. (5) is true for any given stress states, it implies that the creep surface may be represented by a Mises stress surface and the material hardens isotropically. This follows from the fact that creep under the given stress state reduces the strain rate for any other state of stress in an isotropic fashion since the magnitude of the strain rate tensor  $(\frac{1}{2}\dot{\epsilon}_{ij}\dot{\epsilon}_{ij})^{1/2}$  is constant at a given time along a  $J_2$  curve. A strain hardening model can be obtained by expressing  $t$  in terms of the accumulated effective strain as discussed in [13].

The creep surface may be related to the state variable theories, the flow rules of most of which were expressed as:

$$\dot{\epsilon}_{ij} = F_b(J'_2, K) \Sigma_{ij} \quad (6)$$

where  $\Sigma_{ij} = \sigma'_{ij} - \alpha_{ij}$ ,  $J'_2$  is the second invariant of  $\Sigma_{ij}$ , and  $K$  and  $\alpha_{ij}$  are the scalar and the tensorial state variables respectively. These flow rules imply that the strain rate tensor has the same direction as  $\Sigma_{ij}$  and the creep surface defined by constant strain rate magnitude can be represented by  $J'_2 = \text{constant}$ .

Anisotropic creep surfaces may be introduced by (6). Since  $\alpha_{ij}$  defines the center of the creep surface, nonzero values of  $\alpha_{ij}$  result in kinematic movement of the creep surface. Furthermore, squaring both sides of (6) yields  $(\frac{1}{2}\dot{\epsilon}_{ij}\dot{\epsilon}_{ij})^{\frac{1}{2}} = [F_b(J'_2, K)](\frac{1}{2}\Sigma_{ij}\Sigma_{ij})^{\frac{1}{2}} = F_b(J'_2, K)J'_2$ . Thus surfaces of constant  $J'_2$  and  $K$  imply constant magnitudes of strain rate tensors.

Although it is quite impossible to draw any conclusion about the hardening natures of the material from constant stress creep data, Eq. (5) can be evaluated by comparing the creep rates of different creep tests whose stress levels are equated by the Mises relation. According to Eq.(5), the ratio  $\dot{\epsilon}_{11}/\dot{\epsilon}_{12}$  should equal  $2/\sqrt{3}$  for a pure axial creep test and the corresponding pure shear test whose stress levels lie on the same Mises surface. However, a comparison of the values of  $\epsilon_{ij}^+$  and  $\epsilon_{ij}^{+V}$  in Table 3 for the axial and shear tests on the same Mises curve showed that none of these data satisfied this requirement. They actually showed

the opposite tendencies, i.e., shear creep rates were higher than axial creep rates. The data for 304 stainless steel also showed the same thing [9,10,14] .

To eliminate this disagreement,  $F_a(J_2)$  in Eq.5 was replaced by  $F_c$  as a function of maximum shear stress

$\tau_{\max}$  ,

$$\dot{\epsilon}_{ij} = F_c(\tau_{\max})\sigma'_{ij}t^m . \quad (7)$$

Equation (7) shows that vectors  $\dot{\epsilon}_{ij}$  and  $\sigma'_{ij}$  have the same directions, which is normal to a Mises surface. Taking the maximum of the shear stress on the right-hand side of (7) and the maximum of the shear strain rate on the left-hand side shows that the maximum shear strain rates are a function of the maximum shear stress and time only. Thus at any given time the maximum shear strain rates are constant along a Tresca curve. Here the magnitude of the strain rate is defined by the maximum shear strain rate, which in this case is  $[\left(\frac{3}{4}\dot{\epsilon}_{11}\right)^2 + \dot{\epsilon}_{12}^2]^{\frac{1}{2}}$  for combined tension and torsion. If Eq. (7) is true for any given state of stress, it implies that a creep surface defined by normality of the strain rate vector is not the same as that defined by constant strain rate magnitudes, as discussed in [15] . Furthermore, the rate ratio  $\dot{\epsilon}_{11}/\dot{\epsilon}_{12}$  for a pure axial creep test and a pure shear test whose stress levels are the same according to the Tresca relation should be 4/3. Comparing the values of  $\epsilon_{ij}^{+V}$  and  $\epsilon_{ij}^+$  of tests 29

(pure torsion) with those of test 24 (pure tension) which are on the same Tresca curve, see Fig.1, yields ratios which are almost exactly  $4/3$ , i.e., 1.295 for  $\epsilon_{ij}^{+V}$  and 1.33 for  $\epsilon_{ij}^{+}$  respectively. A subsequent section will show that the Tresca relation can describe the whole set of constant stress creep data quite well. This implies that the strain rate magnitudes defined by maximum shear rate are the same at any given time for those creep tests whose stress levels are given by the same Tresca relation. A disadvantage of the Tresca type of expression is that it cannot be derived from a potential theory.

It should be noticed that neither (5) nor (7) can specify exactly the initial creep surface because the initial creep rate is very rapid, infinite as described by the power of time. Also their agreement with constant stress creep data does not guarantee that the material has an isotropic hardening nature. Other more complicated stress histories such as nonproportional loadings are necessary for this determination. However, the degree of agreement of (5) and (7) with data does give some indications of the suitability of using a Mises or Tresca relation to extend the constitutive relations from uniaxial to multiaxial stress states.

#### THE STRESS DEPENDENCE OF $\epsilon^{VE}$ AND $\epsilon^V$

In previous work [2-5], the stress dependences of the

time-dependent components were represented by a third order multiple integral representation combined with creep limits below which creep does not occur or is negligible. However, the current data at stresses as low as 34.5Mpa(5.00ksi) shows that there is creep below the transition previously called a creep limit. Also, the creep behavior below the apparent creep limits is very nearly linear. Therefore, in the following analysis, no creep limits will be included.

The third order multiple integral representation yields the following expressions [2] for the stress-dependent coefficients  $\epsilon_{11}^{+VE}$  and  $\epsilon_{12}^{+VE}$  under constant combined tension and torsion stress, i.e.,

$$\epsilon_{11}^{+VE} = F_1^+ \sigma + F_2^+ \sigma^2 + F_3^+ \sigma^3 + F_4^+ \sigma \tau^2 + F_5^+ \tau^2, \quad (8)$$

$$\epsilon_{12}^{+VE} = G_1^+ \tau + G_2^+ \tau^3 + G_3^+ \sigma \tau + G_4^+ \sigma^2 \tau, \quad (9)$$

where  $F_i^+$  and  $G_i^+$  are constants.

Because of symmetry in tension versus compression,  $F_2^+$  and  $G_3^+$  are zero. Also,  $F_5^+$  is zero since there occurred negligible axial creep strain during pure shear creep tests except for test 42 in which a small amount of axial strain was detected in the tertiary stage, which might be due to the large deformation in shear.

By use of the least squares, the values of  $F_1^+$ ,  $F_3^+$  and  $G_1^+$ ,  $G_2^+$  were determined from pure tension and pure

torsion test data respectively. Then the values of  $F_4^+$  and  $G_4^+$  were determined from combined tension and torsion data. The details of these procedures can be found in [2,16]. The constants for  $\epsilon^{+VE}$  determined through these procedures are shown in Table 4. Expressions (8) and (9) are represented by solid lines for pure axial and pure shear tests and dotted lines for combined tension and torsion tests in Fig. 8.

However, it was found that the coefficients for the  $\epsilon^V$  component ( $\epsilon^{+V}$ ) were not well described by equations like (8) and (9). Apparently terms of higher order than these would be required to describe the stress dependence of  $\epsilon^V$ , which would be impractical. In experimental results for 304 stainless steel [9,10], the data were separated into linear and nonlinear regions to deal with this situation. Here, because of the agreements with tests 24 and 29 as discussed in previous section, Eq.(7) was employed to represent the  $\epsilon^V$  component. Under constant stress,  $\epsilon^V$  can then be expressed by

$$\epsilon_{ij}^V = F(\tau_{\max}) \sigma'_{ij} t^n, \quad (10)$$

where  $\tau_{\max}$  is the maximum shear stress,  $\sigma'_{ij}$  is the stress deviator and  $F(\tau_{\max}) \sigma'_{ij}$  represents the stress dependence of  $\epsilon_{ij}^{+V}$ . The incompressibility of  $\epsilon_{ij}^V$  is a corollary of this expression.

For combined tension  $\sigma$  and torsion  $\tau$  stress states,  $\sigma'_{ij}$  is equal to zero except for  $\sigma'_{11} = (2/3)\sigma$ ,

$\sigma'_{22} = \sigma'_{33} = (-1/3)\sigma$  ,  $\sigma'_{12} = \sigma'_{21} = \tau$  . Also  $\tau_{\max}$  is equal to  $[(\sigma/2)^2 + \tau^2]^{1/2}$  . To check the validity of equation (10),  $\epsilon_{ij}^{+V}$  (in Table 3)/ $\sigma'_{ij}$  was plotted versus  $\tau_{\max}$  , also  $\epsilon_{ij}^+$  (in Table 3)/ $\sigma'_{ij}$  was plotted versus  $\tau_{\max}$  for a possible viscoplastic approach. These plots are shown in Fig. 9 as the lower and the upper data sets respectively. Even though there seemed to be some deviations for combined tension and torsion tests, the data showed a homogeneous relationship in  $F(\tau_{\max})$  . On the other hand, if Eq. 5 was employed, then  $F(\tau_{\max})$  in Eq. 10 should be replaced by  $F(J_2)$  . A plot of  $\epsilon_{ij}^+/\sigma'_{ij}$  vs  $J_2$  would show the invalidity of this expression. For example, tests T26 and A32 are on the same Mises curve, see Fig.1 . Two other pairs T38 and A39, T42 and A40 are also on the same Mises curves. However, their values are not the same as required by  $F$  as a function of  $J_2$  . They are far apart as may be observed in Fig. 9.

The functions  $F(\tau_{\max})$  were found to represent the data best using the following expressions :

for  $\epsilon_{ij}^{+V}$  ,

$$F(\tau_{\max}) = 3.616 \times 10^{-5} \times \{1 + 0.3914 \times \exp [2.108 \times 10^5 \times (\tau_{\max}/G)^2]\} , \\
 \text{percent per MPa - hr}^{0.496} ; \quad (11)$$

and for  $\epsilon_{ij}^+$  ,

$$F(\tau_{\max}) = 6.219 \times 10^{-5} \times \{1 + 0.6433 \times \exp [1.633 \times 10^5 \times (\tau_{\max}/G)^2]\} , \\
 \text{percent per MPa - hr}^{0.407} , \quad (12)$$

where  $G$  is the shear modulus determined in a previous section. Eq. 11 and 12 are shown respectively as the lower and the upper solid lines in Fig. 9.

If the exponential term in (11) or (12) is expanded in a Taylor series and multiplied by  $\sigma'_{ij}$ , the first two terms of Eq. (11) or (12) reduce to the same form as (8) and (9) with  $F_2^+ = F_5^+ = G_3^+ = 0$ . However, in this case, the coefficients for  $\epsilon_{11}^{+V}$  and  $\epsilon_{12}^{+V}$  are not independent of each other because incompressibility was assumed in Eq. 9.

The stress dependences of  $\epsilon_{ij}^{+V}$  represented by  $F(\tau_{\max})\sigma'_{ij}$  are shown in Fig. 10 as the solid lines for pure axial and pure shear tests and as dotted lines for combined tension and torsion tests. The agreement with the test data are quite good.

#### CONCLUSIONS

48 hour creep and recovery data over a wide range of multiaxial stress states showed that creep limits did not exist and that aging effects were negligible up to 300 hours. The time dependence was resolved into recoverable and nonrecoverable components having different time dependences and stress dependences. A third order polynomial in stress was found inadequate to describe the stress dependence of the nonrecoverable component. Creep was symmetrical in tension versus compression. The strain

rate magnitudes defined by maximum shear rate are the same at any given time for those creep tests whose stress levels are the same according to the Tresca relation. The creep behavior at low stresses, which can closely be approximated by a linear relationship, is different from that at high stress.

The stress-strain relations for constant stress creep and recovery employed the modified superposition principle for the recoverable component of strain and a function of the maximum shear stress multiplied by the stress deviator for the nonrecoverable component of strain. A function of the second invariant of the stress deviator (Mises relation) was not applicable.

#### ACKNOWLEDGEMENT

This work was supported by the Army Research Office, Research Grant Number DAAG29-81-K-0138. The material was contributed by the Aluminum Company of America. The authors are grateful to R.M. Reed for assistance in experiments.

## REFERENCES

1. Findley, W.N., Cho, U.W., Ding, J.L., "Creep of Metals and Plastic Under Combined Stresses, A Review," ASME Journal of Engineering Materials and Technology, Vol.101, 1979, p.365.
2. Findley, W.N., and Lai, J.S., "Creep and Recovery of 2618 Aluminum Alloy Under Combined Stress with a Representation by a Viscous-Viscoelastic Model," ASME Journal of Applied Mechanics, Vol.45, Sept.1978, pp.507-514.
3. Lai, J.S., and Findley, W.N., "Creep of 2618 Aluminum Under Step Stress Changes Predicted by a Viscous-Viscoelastic Model," ASME Journal of Applied Mechanics, Vol.47, Mar.1980, pp.21-26.
4. Findley, W.N., and Lai, J.S., "Creep of 2618 Aluminum Under Side Steps of Tension and Torsion and Stress Reversal Predicted by a Viscous-Viscoelastic Model," ASME Journal of Applied Mechanics, Vol.48, 1981, pp.47-54.
5. Lai, J.S., and Findley, W.N., "Simultaneous Stress Relaxation in Tension and Creep in Torsion of 2618 Aluminum at Elevated Temperature," ASME Journal of Applied Mechanics, Vol.49, 1982, pp.19-25.
6. Blass, J.J., and Findley, W.N., "Short Time Biaxial Creep of an Aluminum Alloy with Abrupt Changes of Temperature and State of Stresses," ASME Journal of Applied Mechanics, Vol.38, 1971, pp.489-501.
7. Findley, W.N., and Gjelsvik, A., "A Biaxial Testing Machine for Plasticity, Creep or Relaxation Under Variable Principal Stress Ratios," Proceedings, American Society for Testing and Materials, Vol.62, 1962, pp.1103-1118.
8. Findley, W.N., "A Compressive Creep Machine" ASTM Journal of Testing and Evaluation, Vol.10, July 1982, pp. 179-180.
9. Cho, U.W., and Findley, W.N., "Creep and Creep Recovery of 304 Stainless Steel Under Combined Stress with a Representation by a Viscous-Viscoelastic Model," ASME Journal of Applied Mechanics, Vol.47, No.4, Dec.1980, pp.755-761.
10. Cho, U.W., and Findley, W.N., "Creep and Creep Recovery of 304 Stainless Steel at Low Stresses with Effects of Aging on Creep and Plastic Strains," ASME Journal of Applied Mechanics, Vol.48, pp.785-790.
11. Robotnov, Yu.N., Creep Problems in Structural Members, North-Holland, Amsterdam, 1969.

12. Henderson, J., "An Investigation of Multiaxial Creep Characteristics of Metals," ASME Journal of Engineering Materials and Technology, Vol.101, 1979, p.356.
13. Kraus, H., Creep Analysis ,Wiley, New York (1980).
14. Mark, R., and Findley, W.N., "Concerning a Creep Surface Derived From a Multiaxial Integral Representation for 304 Stainless Steel Under Combined Tension and Torsion," ASME Journal of Applied Mechanics, Vol.45, No.4, Dec. 1978, pp.773-780.
15. Findley, W.N., Lai,J.S., and Nolte, K.G., "Concerning a Creep Surface for an Aluminum Alloy," ASME Journal of Applied Mechanics, Vol.38, Dec.1971, pp. 1091-1094.
16. Findley, W.N., Lai, J.S., and Onaran, K., Nonlinear Creep and Relaxation of viscoelastic Materials, With an Introduction to Linear viscoelasticity , North-holland, Amsterdam, 1976.

Table 1: Chemical Compositions of the Previous and the  
Current Lots of 2618-T61 Aluminum Alloy

Composition wt. percent	Cu	Fe	Mg	Ni	Ti	Si	Mn
previous	2.2	1.1	1.6	1.05	0.07		
current	2.2	0.99	1.55	1.38	0.06	0.27	0.07

Table 2: Numerical results for 2 hour creep and recovery data

Test No.	Tension, $\sigma$		Torsion, $\tau$		Eq. (1)		Eq. (3)		Eq. (4)		
	MPa	(ksi)	MPa	(ksi)	$\epsilon_{ij}^0$	$\epsilon_{ij}^+$	N	$A_{ij}$	$\epsilon_{ij}^{+VE}$	$n_1$	$\frac{E}{\epsilon_{ij}^+}$
					$10^{-4}$	$10^{-5}/hr^N$		$10^{-4}$	$10^{-5}/hr^{n_1}$		$10^{-4}$
T28	0	(0)	27.37	(3.97)	5.720	4.167	0.2318	-2.412	1.704	0.7901	6.162
CT30	62.05	(9.00)	27.37	(3.97)	5.494	4.843	0.2636	0.565	1.554	0.4919	5.687
T29	0	(0)	41.37	(6.00)	8.420	6.922	0.2730	1.643	2.370	0.3337	8.564
CT31	82.74	(12.00)	41.37	(6.00)	8.587	9.134	0.3097	2.757	6.739	0.1322	8.347
A33	34.47	(5.00)	0	(0)	5.186	1.386	0.4131	0.606	1.472	0.3163	5.184
A25	62.05	(9.00)	0	(0)	9.861	3.884	0.3787	1.280	3.509	0.1974	9.807
CA30	62.05	(9.00)	27.37	(3.97)	9.692	5.340	0.3648	1.761	9.256	0.0723	9.154
A24	82.74	(12.00)	0	(0)	12.660	7.380	0.3560	1.797	3.243	0.3712	12.900
CA31	82.74	(12.00)	41.37	(6.00)	12.890	9.698	0.3178	3.029	7.999	0.1593	12.560
CA45	82.74	(12.00)	63.23	(9.17)	12.350	20.030	0.2427	6.204	10.870	0.1773	12.340
T26	0	(0)	63.23	(9.17)	13.000	16.060	0.3162	5.180	11.880	0.1322	12.560
CT45	82.74	(12.00)	63.23	(9.17)	13.580	22.750	0.3043	9.412	20.670	0.0954	12.020
T38	0	(0)	79.22	(11.49)	17.690	33.580	0.2552	12.960	14.660	0.1618	16.600
A32	109.49	(15.88)	0	(0)	16.960	12.910	0.3258	3.569	6.834	0.2931	16.820
A37*	-109.49	(-15.88)	0	(0)	17.250	15.620	0.3235	4.752	7.872	0.1854	16.970
A35**	109.49	(15.88)	0	(0)	16.630	15.050	0.2923	3.328	8.452	0.2372	16.780
A39	137.21	(19.9)	0	(0)	21.380	27.030	0.2983	8.267	14.970	0.1990	21.610
A44*	-137.21	(-19.9)	0	(0)	21.030	32.300	0.2487	8.820	13.290	0.2050	21.170
A43**	137.21	(19.9)	0	(0)	21.370	35.500	0.2399	9.370	25.580	0.1104	20.260
T42	0	(0)	101.35	(14.7)	22.18	90.58	0.2824	220.100	155.800	0.0292	7.456
A40	175.54	(25.46)	0	(0)	28.430	59.490	0.2839	90.17	42.520	0.1088	26.550

\*Compression test

\*\*Aging test

Note: For test 42, the creep duration considered was 0.808 hours.

Table 3: Numerical results for 48 hour creep and recovery data

Test No.	Eq. (1) with N=0.407		Eq. (3) with n <sub>1</sub> =0.223		Eq. (2) n <sub>1</sub> =0.223; n <sub>2</sub> =0.496		Eq. (2) with n <sub>1</sub> =0.223; n <sub>2</sub> =0.496		
	N	$\epsilon_{ij}^0$ 10 <sup>-4</sup>	$\epsilon_{ij}^+$ 10 <sup>-5</sup> /hr <sup>N</sup>	A <sub>ij</sub> 10 <sup>-4</sup>	$\epsilon_{ij}^{+VE}$ 10 <sup>-5</sup> /hr <sup>n<sub>1</sub></sup>	E $\epsilon_{ij}$ 10 <sup>-4</sup>	n <sub>2</sub>	E $\epsilon_{ij} + \epsilon_{ij}^P$ 10 <sup>-4</sup>	$\epsilon_{ij}^{+V}$ 10 <sup>-5</sup> /hr <sup>n<sub>2</sub></sup>
T28	0.4519	5.815	3.245	0.3309	0.763	2.455	0.5701	5.743	1.559
CT30	0.3972	5.624	3.479	0.2593	1.130	2.407	0.4772	5.562	1.733
T29	0.4038	8.580	5.246	0.2936	1.826	3.227	0.4726	8.512	2.723
CT31	0.4115	8.762	7.159	0.1867	2.641	4.169	0.4799	8.686	3.775
A33	0.5757	5.103	2.344	0.2887	0.673	2.052	0.8002	5.030	1.059
A25	0.4247	9.841	4.195	0.3233	1.176	3.637	0.5504	9.718	1.884
CA30	0.4110	9.722	5.020	0.2766	1.495	4.064	0.5223	9.596	2.330
A24	0.4200	12.700	6.969	0.2730	2.199	4.623	0.5080	12.590	3.526
CA31	0.4224	13.010	8.339	0.2094	2.975	5.556	0.5197	12.870	4.203
CA45 <sup>Δ</sup>	0.4513	12.840	14.500	0.2046	6.081	8.775	0.5793	12.660	7.631
T26	0.4324	13.240	13.160	0.1654	5.039	6.981	0.5003	13.150	7.161
CT45 <sup>Δ</sup>	0.4459	13.800	19.690	0.1513	9.109	9.092	0.5393	13.730	11.240
T38 <sup>Δ</sup>	0.2952	18.440	24.540	0.1774	12.810	10.580	0.3366	18.360	14.570
A32	0.4268	17.120	11.020	0.2660	3.850	8.463	0.5421	16.870	5.263
A37*	0.3781	17.570	12.060	0.1531	4.755	6.113	0.4252	17.510	6.614
A35**	0.4022	17.010	10.650	0.1757	3.519	8.021	0.4995	16.770	5.123
A39 <sup>Δ</sup>	0.4572	21.700	22.380	0.1917	8.271	12.800	0.5649	21.480	11.920
A44* <sup>Δ</sup>	0.4042	21.880	22.410	0.1414	9.003	10.670	0.4698	21.810	12.520
A43* <sup>Δ</sup>	0.3798	22.480	22.250	0.1676	8.927	13.390	0.4665	22.230	11.580
T42 <sup>Δ</sup>	0.2437	23.000	89.580	0.0259	219.600	19.320	0.2491	23.130	69.620
A40 <sup>Δ</sup>	0.3055	29.310	49.530	0.0834	89.900	18.710	0.3508	29.200	31.440

\*Compression test

\*\*Aging test

Note: 1. The duration within which data were taken into analysis were 33.083, 17.000, 0.808 and 6.800 hours for the creep steps of tests 45, 38, 42, and 40 respectively. All the others are the whole test durations, i.e. 48 hours for both the creep and the recovery step except for test 42 whose recovery step lasted 36 hours.

2. The elastic responses  $\epsilon_{ij}^E$  from Table 2 were taken into account in computing N and n<sub>2</sub> for tests indicated by  $\Delta$  by including in the data set the elastic strain at t=0 calculated from E and G.

Table 4: Constants for Eq. (7) and (8)

$F_1^+$	$4.634 \times 10^{-7}$ , per MPa-h <sup>n1</sup>	$3.195 \times 10^{-6}$ , per ksi-h <sup>n1</sup>
$F_3^+$	$1.964 \times 10^{-11}$ , per MPa <sup>3</sup> -h <sup>n1</sup>	$6.437 \times 10^{-9}$ , per ksi <sup>3</sup> -h <sup>n1</sup>
$F_4^+$	$1.156 \times 10^{-10}$ , per MPa <sup>3</sup> -h <sup>n1</sup>	$3.789 \times 10^{-8}$ , per ksi <sup>3</sup> -h <sup>n1</sup>
$G_1^+$	$5.938 \times 10^{-7}$ , per MPa-h <sup>n1</sup>	$4.094 \times 10^{-6}$ , per ksi-h <sup>n1</sup>
$G_2^+$	$1.261 \times 10^{-10}$ , per MPa <sup>3</sup> -h <sup>n1</sup>	$4.133 \times 10^{-8}$ , per ksi <sup>3</sup> -h <sup>n1</sup>
$G_4^+$	$3.542 \times 10^{-11}$ , per MPa <sup>3</sup> -h <sup>n1</sup>	$1.161 \times 10^{-8}$ , per ksi <sup>3</sup> -h <sup>n1</sup>

Note:  $F_2^+ = F_5^+ = G_3^+ = 0$ ,  $n_1 = 0.223$

## FIGURE CAPTIONS

Fig.1 : Test numbers and stress surfaces

Fig.2 : Creep strains versus time. Solid lines are Eq.(2); dotted lines are Eq.(1). Numbers identify the tests listed in Table 2 with stress values.

Fig.3 : Recovery strains versus time. Solid lines are Eq.(3). Numbers identify the tests listed in Table 2 with stress values.

Fig.4 : Creep strains versus time. Solid lines are Eq.(2); dotted lines are Eq.(1). Numbers identify the tests listed in Table 2 with stress values.

Fig.5 : Recovery strains versus time. Solid lines are Eq.(3). Numbers identify the tests listed in Table 2 with stress values.

Fig.6 : Creep and recovery strains versus time for tests 40 and 42; Solid lines are Eq.(2) for creep, Eq.(3) for recovery; dotted lines are Eq.(1). Numbers identify the tests listed in Table 2 with stress values.

Fig.7 :  $\epsilon_{ij}^{\circ}$  and  $\epsilon_{ij}^E$  in Table 2 versus stress.

Fig.8 :  $\epsilon_{ij}^{+VE}$  versus stress. Solid lines and dotted lines represent the multiple integral representations with the constants shown in Table 4.

Fig.9 :  $\epsilon_{ij}^{+V}/\sigma'_{ij}$  and  $\epsilon_{ij}^{+}/\sigma'_{ij}$  versus maximum shear stress.

The upper and the lower solid lines represent Eq. (12) and (11) respectively.

Fig.10 :  $\epsilon_{ij}^{+V}$  versus stress. The solid lines and the dotted lines represent  $F(\tau_{\max})\sigma'_{ij}$  with  $F(\tau_{\max})$  expressed by Eq. (11)

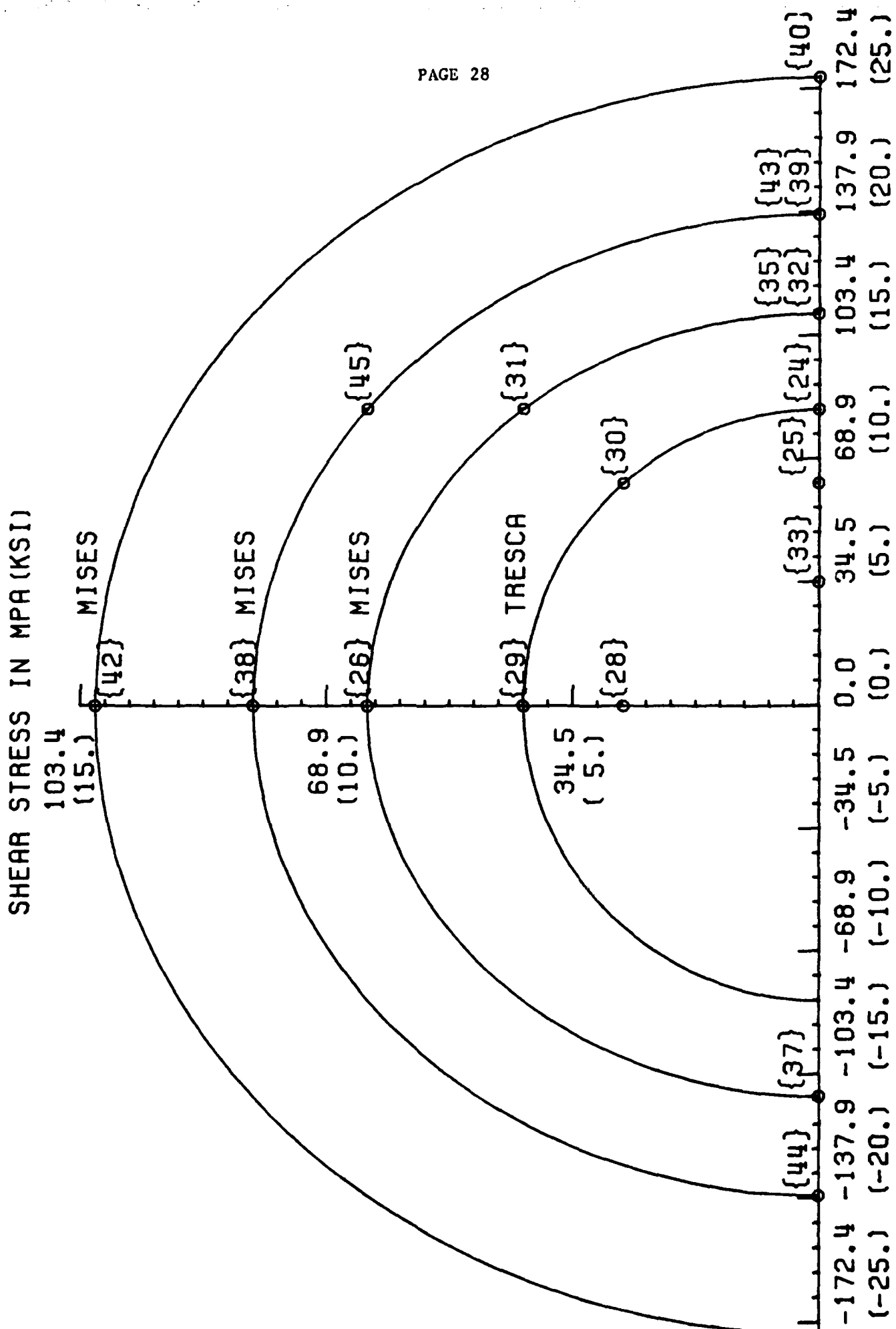


FIG. 1

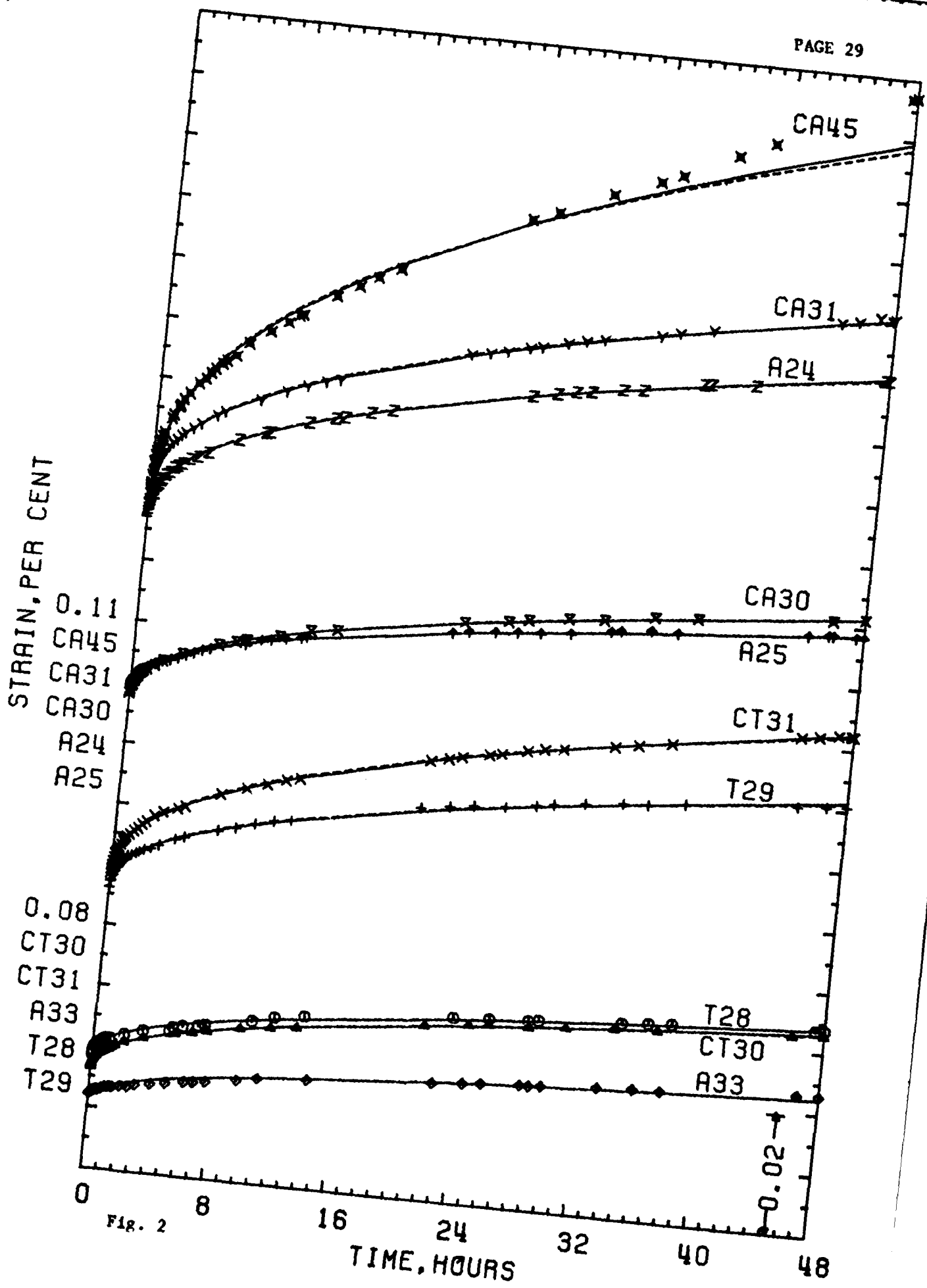


Fig. 2

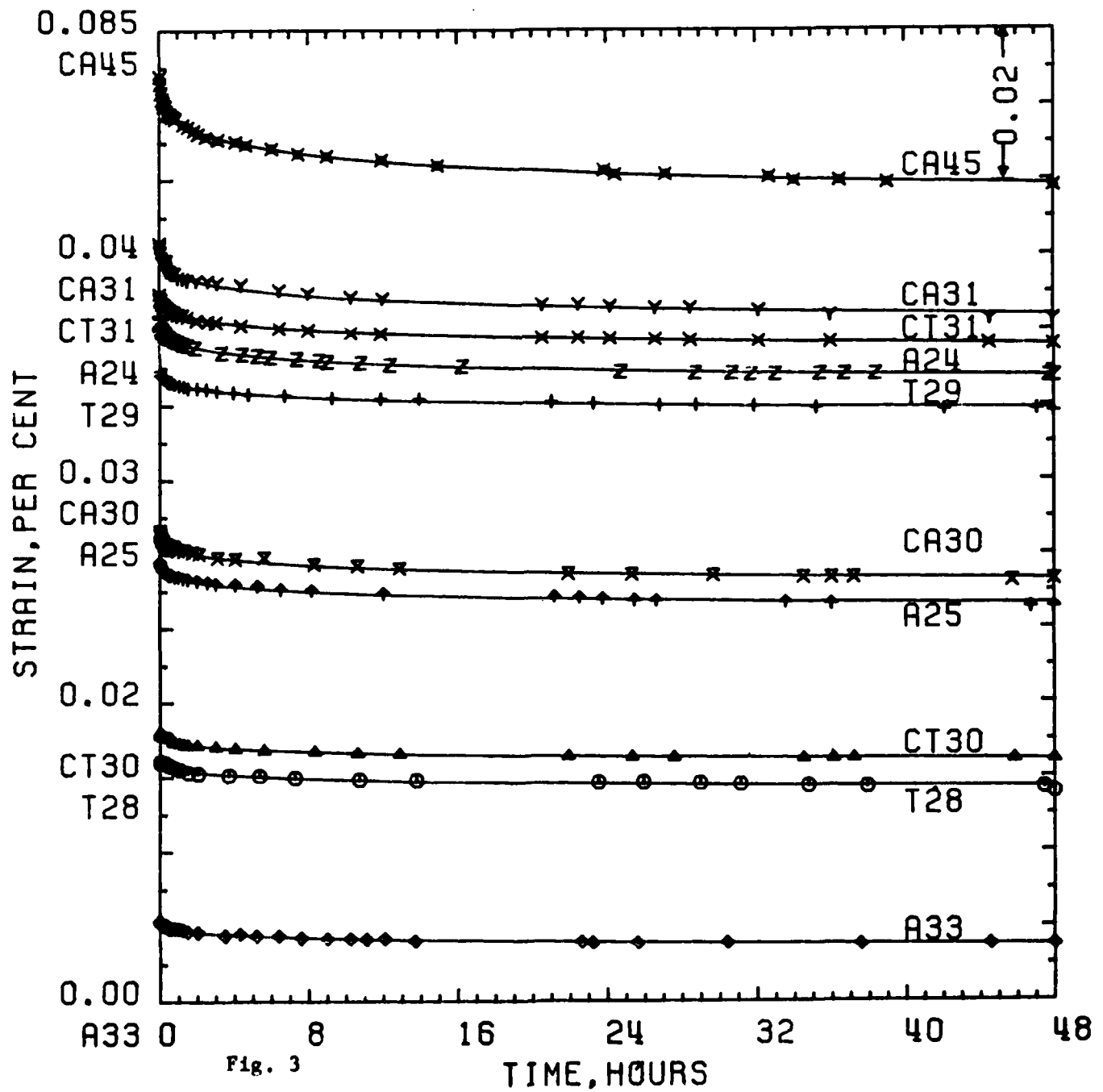


Fig. 3

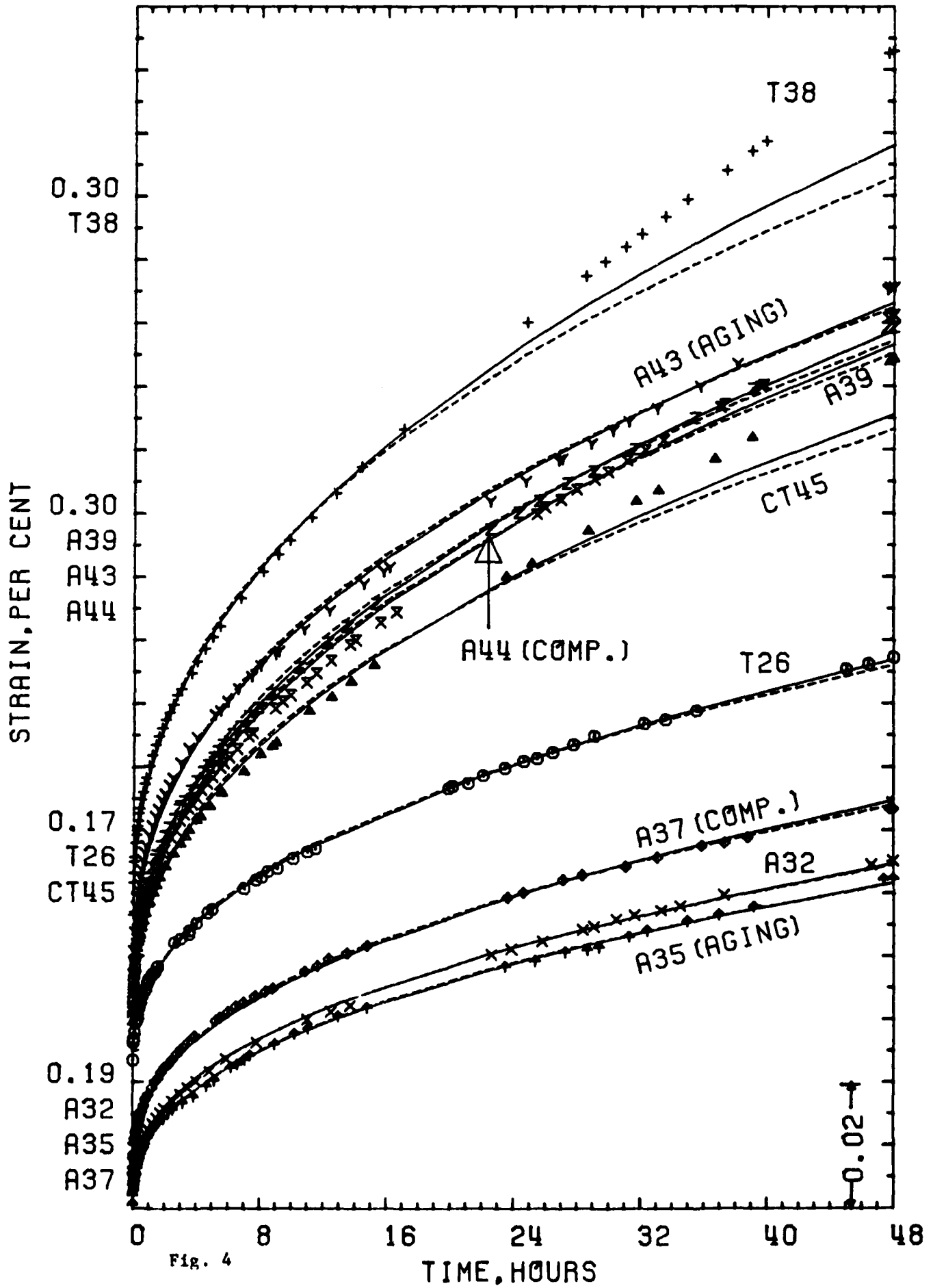


Fig. 4

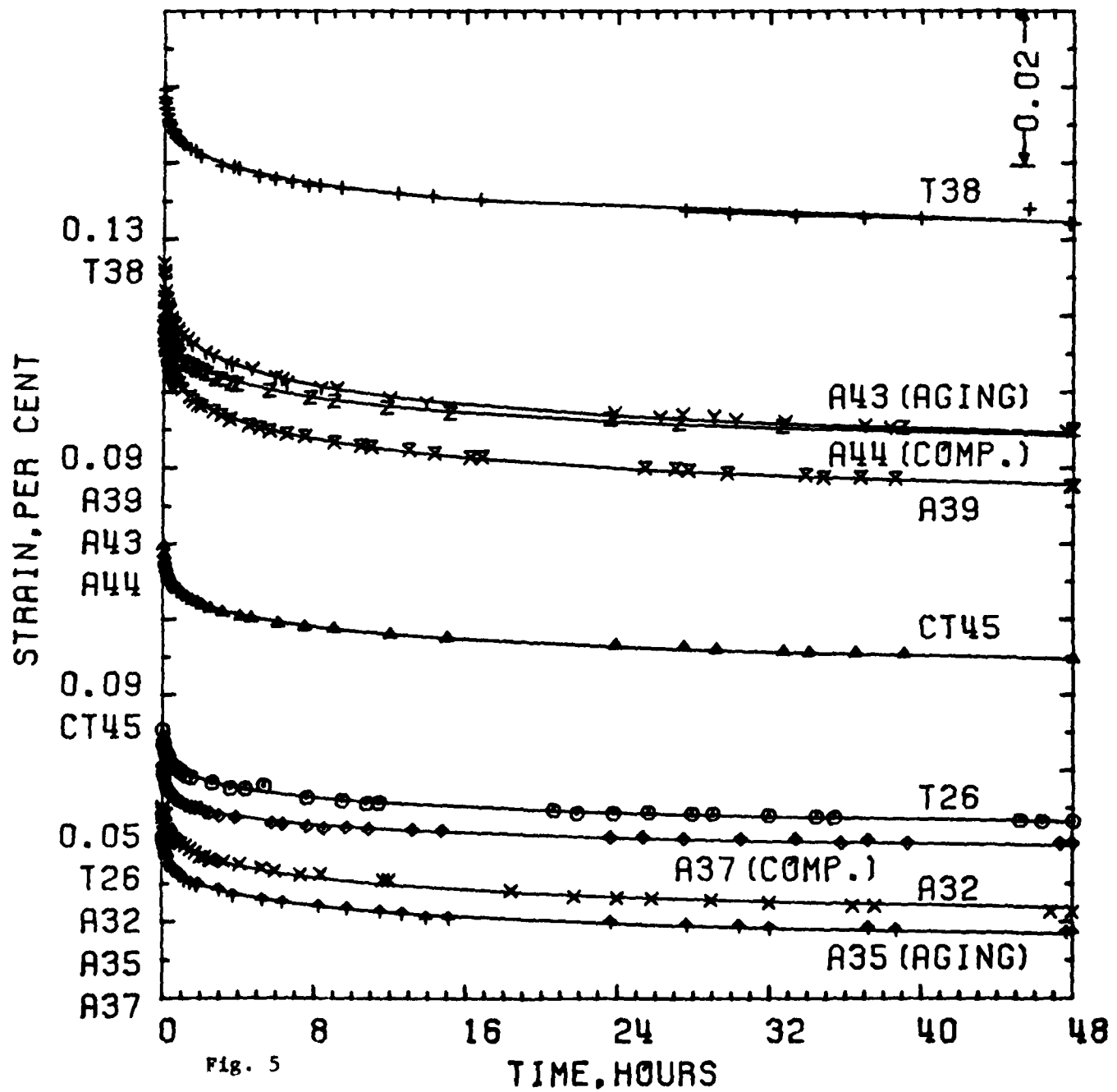


Fig. 5

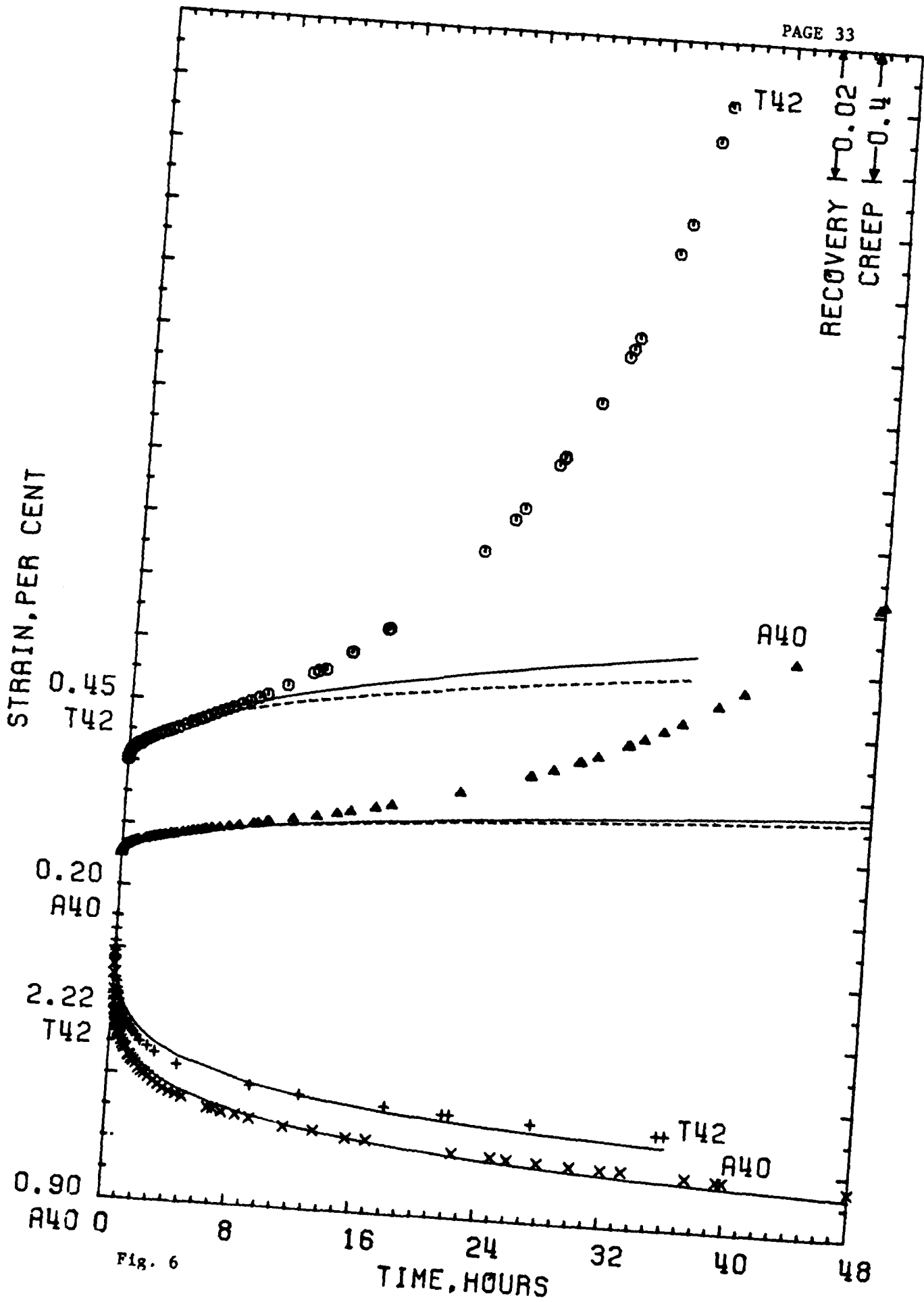


Fig. 6

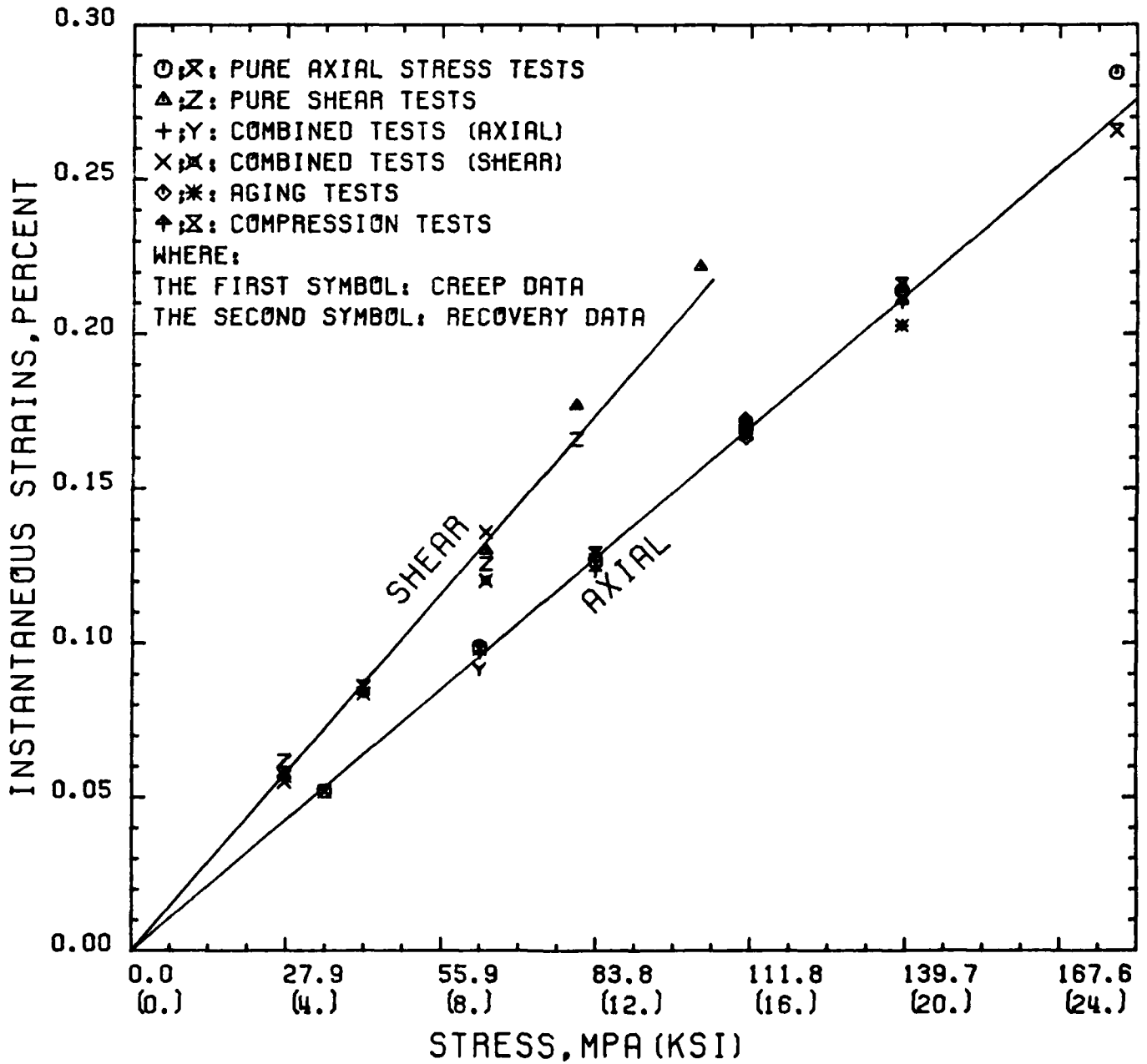


Fig. 7

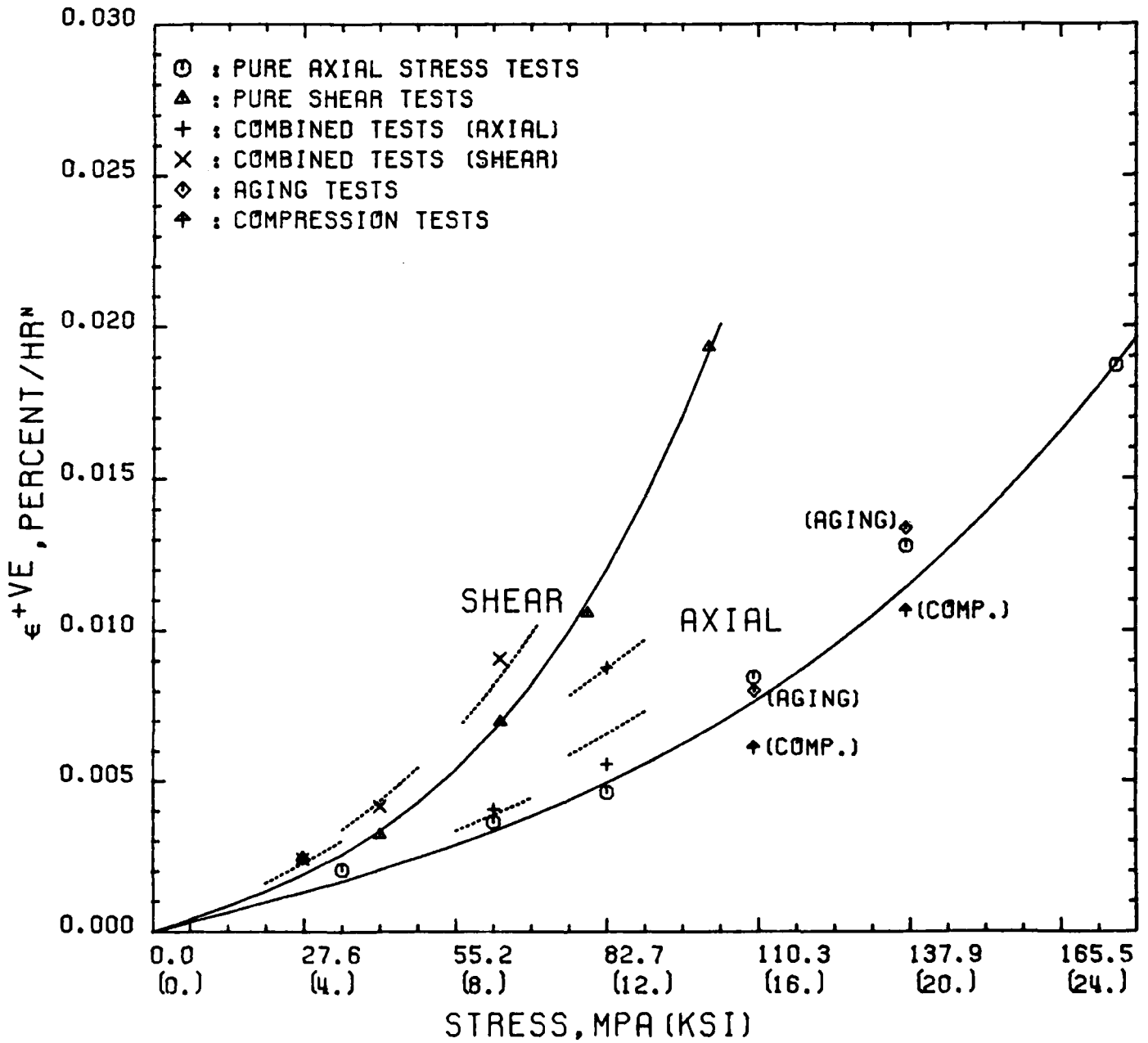


Fig. 8

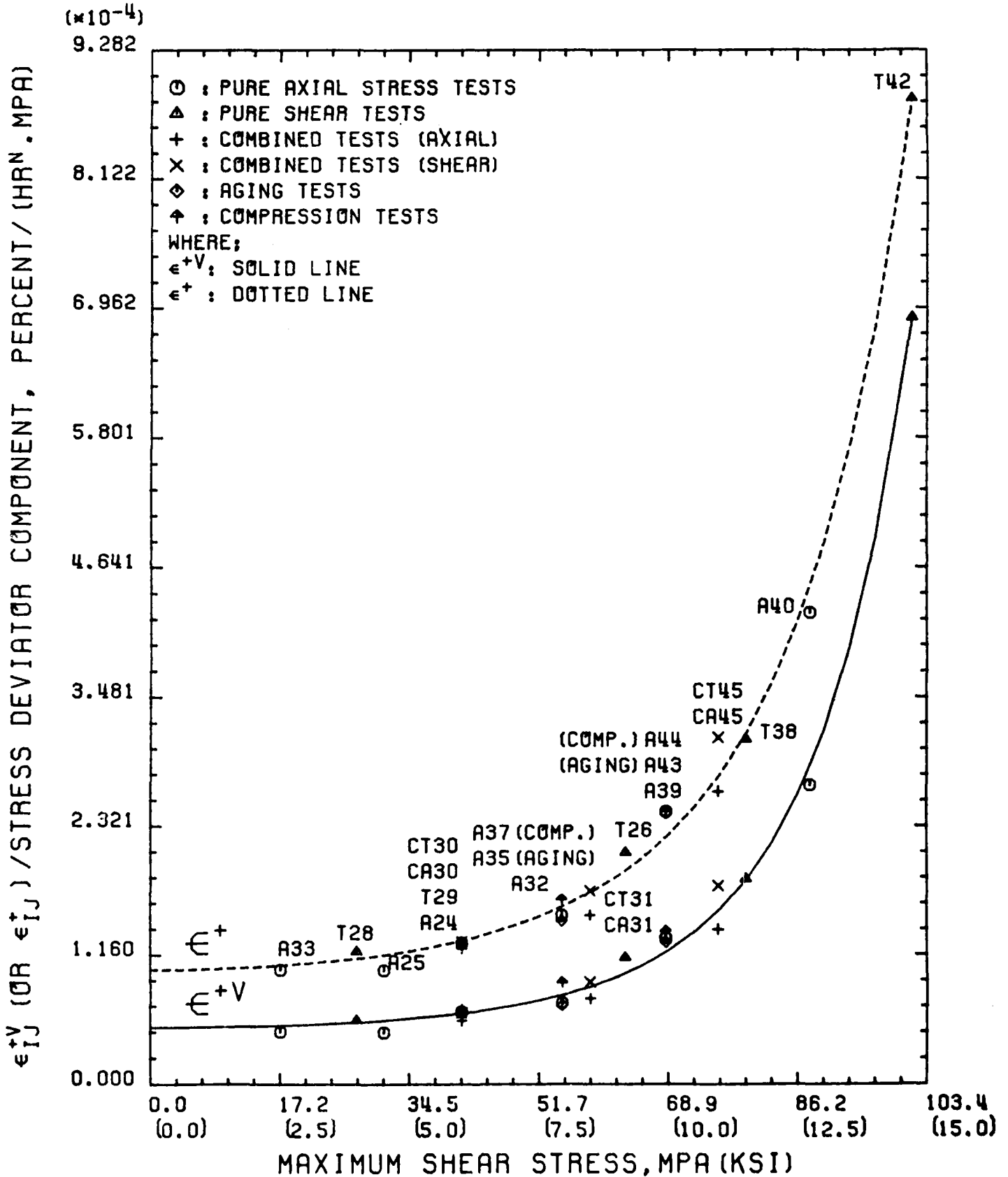


Fig. 9

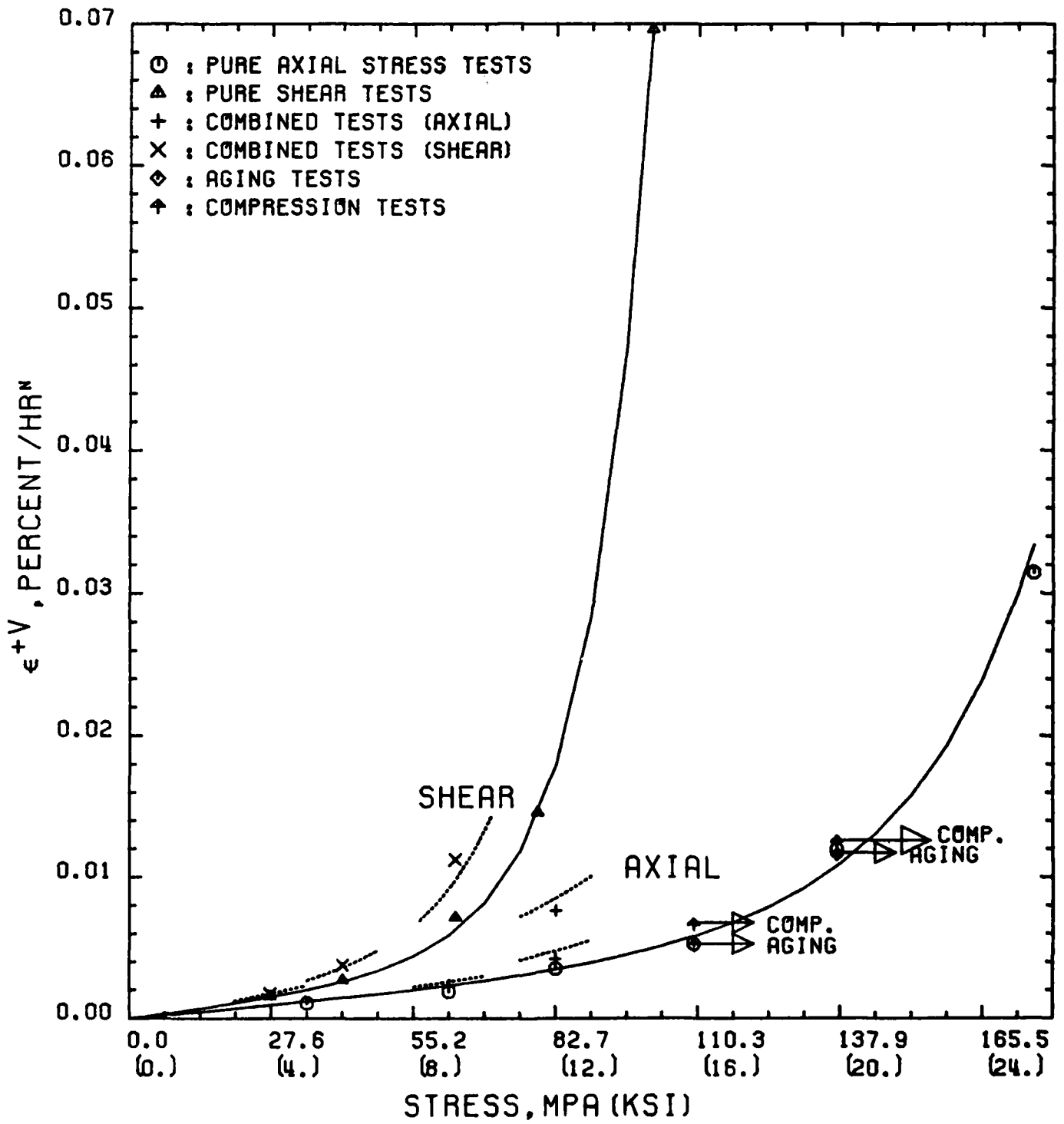


Fig. 10

Te N T2 CT T2 CT A3 A2 CA A2 CA T2 CT T3 A3 A3 A3 A4 A4 T4 A4 \*C #1

END

FILMED

3-83

DTIC